IEEE Access
Multidisciplinary | Rapid Review | Open Access Journal

Received June 8, 2021, accepted July 4, 2021, date of publication July 12, 2021, date of current version July 20, 2021.

Digital Object Identifier 10.1109/ACCESS.2021.3096233

Robust Voltage Stabilization Controller for Uncertain DC Microgrids

JUWON LEE[1], HYO-SUNG AHN[2], (Senior Member, IEEE), AND JUHOON BACK[1], (Member, IEEE)

[1]School of Robotics, Kwangwoon University, Seoul 01897, South Korea
[2]School of Mechanical Engineering, Gwangju Institute of Science and Technology (GIST), Gwangju 61005, South Korea

Corresponding author: Juhoon Back (backhoon@kw.ac.kr)

This work was supported in part by the National Research Foundation of Korea (NRF) grant funded by the Korea Government (MSIT) under Grant 2019R1A4A1029003, and in part by the Korea Institute of Energy Technology Evaluation and Planning (KETEP) grant funded by the Korea Government (MOTIE) (Graduate Track for Core Technologies of Wind Power System Engineering) under Grant 20204030200010.

ABSTRACT In this paper, we propose a new voltage stabilizing controller for a DC microgrid. The microgrid under consideration is composed of Distributed Generation Units (DGUs), power lines, and local loads. The parameters of DGUs and power lines are assumed to be unknown but belong to known bounded sets and the loads, which are modeled by constant current loads, are assumed to be unknown. The proposed controller adopts the disturbance observer based controller which is known to be robust against parameter uncertainties and external disturbances. One benefit of this controller is to make the real uncertain closed-loop system behave like a nominal model, and in this work this nominal model is a desired dynamics relating the voltage reference and output voltages of DGUs. A rigorous stability proof is provided and the results are validated through numerical simulations.

INDEX TERMS DC microgrids, voltage control, robust control.

I. INTRODUCTION

In recent years, the rapid development of renewable energy sources such as photovoltaics, wind power systems, etc. has increased the interest on microgrids among not only power systems society but also control community. A microgrid is a small-scale power generation system composed of Distributed Generation Units (DGUs), power lines, loads, etc. It can operate as a part of the main grid or as an independent power generation source in emergency situations. For details, see the recent reviews [1]–[3] and references therein. Although most of the research is concentrated on AC microgrids, research works on DC microgrids are also expanding because of the advances in the renewable DC sources, DC loads, and energy storage systems (ESS) [4]–[6].

A well-known solution for the DC microgrid control is a hierarchical control structure that is composed of primary, secondary, and tertiary control [7], [8]. The tertiary control manages the power flow among the main grid and DC microgrids. The secondary control performs a load sharing that all DGUs efficiently share their load demands while assisting the primary control. The primary control preforms voltage stabilization (or voltage regulation) so that the output voltage of each DGU is regulated at its reference.

In the conventional hierarchical control [7], a common solution for the primary control is the droop control method, where each DGU imposes a virtual impedance called droop gain. The output voltage reference is reduced linearly when the output current increases and the reduction rate is related to the droop gain. The voltage stabilization as well as the load sharing is done by adjusting this gain. Although the droop control is widely employed as a decentralized control method, it has limitations, voltage deviation and current sharing inaccuracy, which are mainly due to the voltage drop caused by the power line impedance [9], [10]. In order to overcome these drawbacks, several solutions have been proposed in [10]–[12]. In [10], proportional–integral (PI) controllers using averaged current and averaged voltage have been introduced to improve the performance of droop control, where the averages are computed through a fully connected low-bandwidth communication. In [11], [12], the authors proposed a robust DC voltage observer employing a dynamic consensus algorithm. The observer corrects the local voltage set points using information from the neighboring DGUs, and

The associate editor coordinating the review of this manuscript and approving it for publication was Akshay Kumar Saha.

a current regulator is used to improve the current sharing accuracy by comparing the local current with its neighbors.

Recently, alternative decentralized control strategies that are free of droop control have been proposed [13]–[17]. In [13], [14], a primary controller that employs the decentralized multivariable PI controller has been introduced, where the local control gains are computed using Linear Matrix Inequalities (LMIs). Since only limited information is required for the controller, i.e., information on its own DGU and the power lines connected to it [13] or the DGU only [14], the controller is capable of Plug-and-Play (PnP) operation. A consensus-based secondary controller is presented in [15] where a DC microgrid with ZIP (constant impedance, constant current, and constant power) loads is considered. The proposed controller sits atop a primary control that does voltage stabilization, and uses information exchanged over a communication network to perform load sharing. In [16], [17], the authors proposed an integrated controller that achieves voltage stabilization and load sharing at the same time. A consensus-based control scheme is proposed to deal with unknown current loads in [16]. In [17], a distributed coordinate tracking algorithm with a virtual leader has been proposed to achieve the two objectives. In this paper, we propose a new voltage stabilization controller which adopts the disturbance observer (DOB) [18]–[20]. The microgrid under consideration is assumed to have uncertainties in the parameters of DGUs and the resistive-inductive (RL) power lines, and be subject to unknown constant current loads. Main contributions of this paper are summarized below.

1) The proposed control requires the local voltage measurement only. Notably, it achieves the voltage stabilization without using the local current, which is required in [13]–[15].

2) The proposed controller enhances the robustness against the model uncertainties of DGUs and power lines, and the size of unknown loads. In addition, the robust stability of closed-loop system is rigorously analyzed considering parameter uncertainties. This is in contrast to [13], [14], which do not consider parameter uncertainties explicitly.

3) The performance regarding the voltage convergence can be assignable by choosing the desired dynamics of DGU. This is one of main benefits that the disturbance observer based controller provides. It is noted that it is not required to redesign the controller when the desired convergence performance is modified; the controller remains the same and one can just change the desired nominal model while in most cases including [15] the controller should be redesigned.

The remainder of this paper is organized as follows. The problem is formulated in Section II. In Section III, we explain the proposed controller scheme and analyze the stability of the whole closed-loop system. In Section IV, simulation results are presented to verify the proposed controller. Finally, Section V concludes the paper.

Notation: I_k denotes the identity matrix of dimension k. $0_k \in \mathbb{R}^k$ represents a column vector with all components being 0. $1_k \in \mathbb{R}^k$ represents a column vector with all components being 1. $diag\{d^1, \ldots, d^n\}$ denotes the $n \times n$ diagonal matrix whose (k,k)-th component is given by d_k. A polynomial $P(s) = s^n + a_{n-1}s^{n-1} + \cdots + a_0$ is called a Hurwitz polynomial if each root of $P(s)$ has a negative real part. For a matrix $A \in \mathbb{R}^{n\times m}$, A_i denotes the i-th row vector of A.

II. PROBLEM SETUP

We consider a DC microgrid that contains n Distributed Generation Units (DGUs) which are connected through m RL power lines. The electrical scheme of DGU i and power line k is represented in Fig.1. DGU i is composed of a DC voltage source, a Buck converter, a RLC filter, and a local DC load which is connected to the Point of Common Coupling (PCC). We assume that the local DC load is an unknown constant current load (I_L^i).

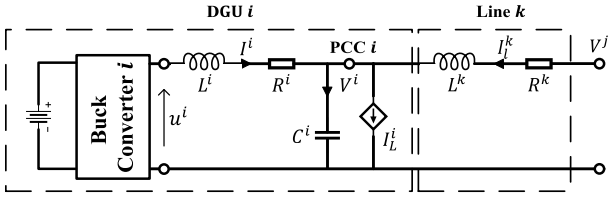

FIGURE 1. Electrical scheme of DGU *i* and power line *k* for a DC microgrid.

We consider an undirected graph $\mathcal{G} = \{\mathcal{N}, \mathcal{E}\}$ where $\mathcal{N} = \{1, \ldots, n\}$ is the node set associated to the set of DGUs and $\mathcal{E} = \{1, \ldots, m\}$ is the edge set associated to the set of power lines interconnecting DGUs. To each edge, say edge $k \in \mathcal{E}$, we assign a direction of current through the power line. Then, we can define the incident matrix $\mathcal{B} \in \mathbb{R}^{n\times m}$ associated to the graph $\mathcal{G}$ whose component $\mathcal{B}_{ik}$ is defined as $+1$ if the current through the power line k enters DGU i, -1 if the current comes from DGU i, and 0 otherwise. With the incidence matrix $\mathcal{B}$ and the matrix $R_l = diag\{R_l^1, \ldots, R_l^m\}$, we define the Laplacian matrix $\mathcal{L} = \mathcal{B}R_l^{-1}\mathcal{B}^\top \in \mathbb{R}^{n\times n}$ which encodes the admittance among DGUs and it is readily seen that $\mathcal{L}$ is a symmetric positive semi-definite matrix.

Now we consider the dynamics of DGU i and power line k. Let I^i, V^i, u^i, and I_L^i be the output current, the output voltage, the control input, and the unknown constant current load of DGU i. The current through power line k is denoted by I_l^k. Define $I_l = \begin{bmatrix} I_l^1 & \cdots & I_l^m \end{bmatrix}^\top \in \mathbb{R}^m$. Then, the dynamics of DGU i is given by

$$\begin{aligned} L^i \dot{I}^i &= -R^i I^i - V^i + u^i \\ C^i \dot{V}^i &= I^i + \mathcal{B}_i I_l - I_L^i \end{aligned} \tag{1}$$

where i denotes DGU's id, and the parameters R^i, L^i, and C^i are the resistance, inductance, and capacitance of DGU i, respectively.

Define $V = \begin{bmatrix} V^1 & \cdots & V^n \end{bmatrix}^\top \in \mathbb{R}^n$. Then, the dynamics of power line k is given by

$$L_l^k \dot{I}_l^k = -R_l^k I_l^k - (\mathcal{B}^\top)_k V \tag{2}$$

where k denotes power line's id, and the parameters L_l^k and R_l^k are the inductance and resistance of power line k, respectively.

We assume that L_l^k is sufficiently small so that the dynamics (2) is reduced to the quasi-stationary line (QSL) model [13] given by

$$I_l^k = -\frac{1}{R_l^k}(\mathcal{B}^\top)_k V. \tag{3}$$

Applying (3), the dynamics of DGU i becomes

$$\begin{aligned} L^i \dot{I}^i &= -R^i I^i - V^i + u^i \\ C^i \dot{V}^i &= I^i - \mathcal{L}_i V - I_L^i. \end{aligned} \tag{4}$$

We would like to allow that heterogeneous DGUs can join the DC microgrid and avoid using exact parameters of DGUs. Moreover, only partial information on the whole circuit network $\mathcal{L}$ will be used to derive the proposed controller. This is intended to gain robustness against parameter uncertainty and network topology. Precisely, we make the following assumption on the measurement, parameters of DGU, and the circuit network.

Assumption 1: For DGU i, the state variable V^i is available for feedback and the bounds of the parameters such that $R^i \in [R_{\min}, R_{\max}]$, $L^i \in [L_{\min}, L_{\max}]$, and $C^i \in [C_{\min}, C_{\max}]$ are known. And the bounds of the eigenvalues of the matrix $\mathcal{L}$ are also known such that $0 \le \mathcal{L} \le \sigma_{\max} I_n$.

The objective of this paper is to design a robust voltage stabilization controller such that all voltages of DGUs converge to its reference value, i.e.,

$$\lim_{t\to\infty} V^i(t) = V_{\text{ref}}, \quad i = 1, \dots, n \tag{5}$$

and all signals in the closed-loop system are bounded.

III. ROBUST VOLTAGE STABILIZATION CONTROLLER

A. STRUCTURE OF LOCAL CONTROLLER

In order to derive a robust controller, we first rewrite the dynamics (4) of DGU i with the state variable $x_1^i = V^i$ and $x_2^i = \dot{V}^i$, namely

$$\begin{aligned} \dot{x}_1^i &= x_2^i \\ \dot{x}_2^i &= -\phi_1^i x_1^i - \phi_2^i x_2^i + g_1^i u^i + d_{\text{ext}}^i \\ d_{\text{ext}}^i &= -\phi_3^i \mathcal{L}_i x_1 - \phi_4^i \mathcal{L}_i x_2 - g_2^i I_L^i \end{aligned} \tag{6}$$

where $\phi_1^i = \frac{1}{C^i L^i}$, $\phi_2^i = \frac{R^i}{L^i}$, $\phi_3^i = \frac{R^i}{C^i L^i}$, $\phi_4^i = \frac{1}{C^i}$, $g_1^i = \frac{1}{C^i L^i}$, $g_2^i = \frac{R^i}{C^i L^i}$, $x_1 = \begin{bmatrix} x_1^1 & \cdots & x_1^n \end{bmatrix}^\top \in \mathbb{R}^n$, and the vector $x_2 \in \mathbb{R}^n$ is similarly defined. It is noted that $\phi_1^i, \dots, \phi_4^i, g_1^i$, and g_2^i are unknown constants. The term d_{ext}^i is composed of the terms that explain the interaction between DGU i and other DGUs joining the microgrid, and the current load. Since d_{ext}^i is not known, we can regard it as an external disturbance.

In addition to the external disturbance, we also have model uncertainty $(\phi_1^i, \phi_2^i, g_1^i)$ that comes from unknown parameters R^i, L^i, and C^i. If we define nominal (or desired) values of ϕ_1^i, ϕ_2^i, and g_1^i, denoted by $\bar{\phi}_1, \bar{\phi}_2$, and $\bar{g}_1$, then the dynamics of x_2^i can be expressed as

$$\dot{x}_2^i = -\bar{\phi}_1 x_1^i - \bar{\phi}_2 x_2^i + \bar{g}_1 u^i + d_{\text{mdl}}^i + d_{\text{ext}}^i \tag{7}$$

where $d_{\text{mdl}}^i = (\bar{\phi}_1 - \phi_1^i)x_1^i + (\bar{\phi}_2 - \phi_2^i)x_2^i + (g_1^i - \bar{g}_1)u^i$.

If we can compensate the external disturbance d_{ext}^i and the model uncertainty d_{mdl}^i successfully so that the dynamics of DGU i becomes a desired one described by

$$\begin{aligned} \dot{\bar{x}}_1 &= \bar{x}_2 \\ \dot{\bar{x}}_2 &= -\bar{\phi}_1 \bar{x}_1 - \bar{\phi}_2 \bar{x}_2 + \bar{g}_1 u_r, \end{aligned} \tag{8}$$

then we have $\lim_{t\to\infty}(\bar{x}_1(t), \bar{x}_2(t)) = (V_{\text{ref}}, 0)$ provided that the system is stable and $u_r = (\bar{\phi}_1/\bar{g}_1)V_{\text{ref}}$. In what follows, we let $u_r = (\bar{\phi}_1/\bar{g}_1)V_{\text{ref}}$. It is noted that $\bar{x}_1$ and $\bar{x}_2$ are used instead of x_1 and x_2 in order to emphasize that the dynamics (8) is the *desired* dynamics that we want to make DGU i behave like.

In fact, we can achieve the objective described above by employing the disturbance observer based controller [19], [20], of which the basic idea can be explained as follows. Firstly the system (6) is expressed as

$$y^i(s) = P^i(s)(u^i(s) + d^i(s)) \tag{9}$$

where $u^i(s)$, $d^i(s)$, and $y^i(s)$ are Laplace transformed signals of $u^i(t)$, $d_{\text{ext}}^i(t)/g_1^i$, and $x_1^i(t)$, respectively, and $P^i(s)$ is the transfer function of the DGU i, i.e., $P^i(s) = g_1^i/(s^2 + \phi_2^i s + \phi_1^i)$. Similarly, let $P_{\text{nom}}(s)$ be the transfer function of the nominal system (8) so that $\bar{y}(s) = P_{\text{nom}}(s)u_r(s)$, where $\bar{y}(s)$ and $u_r(s)$ are Laplace transformed signals of $\bar{x}_1(t)$ and $u_r(t)$, respectively, and $P_{\text{nom}}(s) = \bar{g}_1/(s^2 + \bar{\phi}_2 s + \bar{\phi}_1)$.

Now, we rewrite the system (9) as

$$y^i(s) = P_{\text{nom}}(s)(u^i(s) + \mathsf{d}^i(s)) \tag{10}$$

where $\mathsf{d}^i(s) = P_{\text{nom}}^{-1}(s)P^i(s)(u^i(s) + d^i(s)) - u^i(s)$. If the unknown term $\mathsf{d}^i(s)$ can be estimated successfully, then the control input given by $u^i(s) = u_r(s) - \mathsf{d}^i(s)$ will make the uncertain system (9) become $y^i(s) = P_{\text{nom}}(s)u_r(s)$, i.e., the objective is achieved.

One way to estimate $\mathsf{d}^i(s)$ is to find an estimate of $u^i(s) + \mathsf{d}^i(s)$ and subtract a filtered signal of $u^i(s)$ from it. Precisely, let $u_p^i(s) = u^i(s) + \mathsf{d}^i(s)$. Then, from (10), one has $u_p^i(s) = P_{\text{nom}}^{-1}(s)y^i(s)$. Since $P_{\text{nom}}^{-1}(s)$ is not proper, we introduce a filter $Q(s)$ to compose $\hat{u}_p^i(s) = P_{\text{nom}}^{-1}(s)Q(s)y^i(s)$, which is an estimate of $u_p^i(s)$. We choose

$$Q(s) = \frac{\alpha_0}{(\tau s)^2 + \alpha_1(\tau s) + \alpha_0} \tag{11}$$

where α_1, α_0, and τ are design parameters to be determined later, and construct an estimate of $\mathsf{d}^i(s)$, denoted by $\hat{\mathsf{d}}^i(s)$, as

$$\begin{aligned} \hat{\mathsf{d}}^i(s) &= \hat{u}_p^i(s) - Q(s)u^i(s) \\ &= P_{\text{nom}}^{-1}(s)Q(s)y^i(s) - Q(s)u^i(s). \end{aligned} \tag{12}$$

It is noted that $Q(s)u^i(s)$ rather than $u^i(s)$ is used in (12). In fact, this is to make the input $u^i(s)$ well defined. Suppose $u^i(s)$ is used, i.e., $\hat{\mathsf{d}}^i(s) = \hat{u}_p^i(s) - u^i(s)$. Recalling that $u^i(s) = u_r(s) - \hat{\mathsf{d}}^i(s)$, one has $u^i(s) = u_r(s) - \hat{u}_p^i(s) + u^i(s)$, which implies that $u^i(s)$ is not defined.

The estimate of $\mathsf{d}^i(t)$ is typically implemented by using two identical filters $Q(s)$ [19]. In this paper, we employ a reduced

implementation developed in [20]. From the structure of the involved transfer functions, it follows that

$$\begin{aligned}\hat{\mathsf{d}}^i(s) &= \frac{\frac{\alpha_0}{\tau^2}(s^2+\bar{\phi}_2\, s+\bar{\phi}_1)}{\bar{g}_1(s^2+\frac{\alpha_1}{\tau}s+\frac{\alpha_0}{\tau^2})}y^i(s) - \frac{\frac{\alpha_0}{\tau^2}}{s^2+\frac{\alpha_1}{\tau}s+\frac{\alpha_0}{\tau^2}}u^i(s)\\ &= \frac{(\bar{\phi}_2-\frac{\alpha_1}{\tau})s+(\bar{\phi}_1-\frac{\alpha_0}{\tau^2})}{s^2+\frac{\alpha_1}{\tau}s+\frac{\alpha_0}{\tau^2}}\frac{\alpha_0}{\tau^2}\frac{1}{\bar{g}_1}y^i(s)\\ &\quad -\frac{1}{s^2+\frac{\alpha_1}{\tau}s+\frac{\alpha_0}{\tau^2}}\frac{\alpha_0}{\tau^2}u^i(s)+\frac{\alpha_0}{\tau^2}\frac{1}{\bar{g}_1}y^i(s),\end{aligned}$$

from which we obtain a state space realization of the controller (regarding u^i and $\frac{1}{\bar{g}_1}y^i = \frac{1}{\bar{g}_1}x_1^i$ as inputs and treating the last signal as the direct transmission term)

$$\begin{aligned}\dot{q}^i &= A_{q\tau}q^i + \frac{\alpha_0}{\tau^2}B_{q\tau}\begin{bmatrix}u^i\\ \frac{1}{\bar{g}_1}x_1^i\end{bmatrix}\\ \hat{\mathsf{d}}^i &= -q_1^i + \frac{\alpha_0}{\tau^2}\frac{1}{\bar{g}_1}x_1^i\\ u^i &= u_r - \hat{\mathsf{d}}^i\end{aligned} \tag{13}$$

where the matrices $A_{q\tau}$ and $B_{q\tau}$ are given by

$$A_{q\tau} = \begin{bmatrix}-\frac{\alpha_1}{\tau} & 1\\ -\frac{\alpha_0}{\tau^2} & 0\end{bmatrix},\quad B_{q\tau} = \begin{bmatrix}0 & -\bar{\phi}_2+\frac{\alpha_1}{\tau}\\ 1 & -\bar{\phi}_1+\frac{\alpha_0}{\tau^2}\end{bmatrix}.$$

Fig. 2 shows the controller (13) which serves as the robust voltage stabilizer for DGU i. The design parameters α_0, α_1 and τ are determined to ensure the stability of the closed-loop system and it will be addressed in the next subsection. It is noted that the main benefit of using this reduced implementation is that the stability analysis is substantially simplified compared to the case with the conventional implementation.

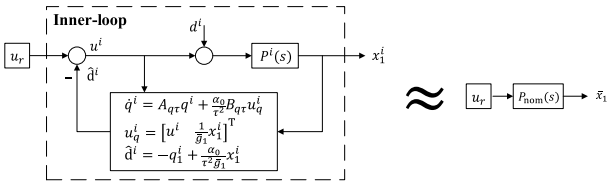

FIGURE 2. **Proposed robust voltage stabilization controller.**

B. STABILITY ANALYSIS OF THE CLOSED-LOOP DC MICROGRID

In order to investigate the stability of the closed-loop system involving the controller (13), for $i = 1, \ldots, n$, we define the following variables.

$$\begin{aligned}\eta_1^i &= g_1^i\left(q_1^i - \frac{\alpha_0}{\tau^2\bar{g}_1}x_1^i\right)\\ \eta_2^i &= \tau\dot{\eta}_1^i = g_1^i\tau\left(\dot{q}_1^i - \frac{\alpha_0}{\tau^2\bar{g}_1}x_2^i\right).\end{aligned} \tag{14}$$

It is noted that η_1^i is nothing but $-\hat{\mathsf{d}}^i$ multiplied by g_1^i. Hence, the control input of DGU i is written as

$$u^i = (1/g_1^i)\eta_1^i + (\bar{\phi}_1/\bar{g}_1)V_{\text{ref}}. \tag{15}$$

We also define variables that describe the difference between the states of DGU i and their nominal counterparts.

$$\begin{aligned}&e_{x,1}^i = x_1^i - \bar{x}_1, \quad e_{x,2}^i = x_2^i - \bar{x}_2\\ &e_{x,1} = \begin{bmatrix}e_{x,1}^1 & \cdots & e_{x,1}^n\end{bmatrix}^\top, \quad e_{x,2} = \begin{bmatrix}e_{x,2}^1 & \cdots & e_{x,2}^n\end{bmatrix}^\top.\end{aligned}$$

Lemma 1: Let $\tilde{\phi}_1^i = \phi_1^i - \bar{\phi}_1$ and $\tilde{\phi}_2^i = \phi_2^i - \bar{\phi}_2$. With the new coordinates η_1^i, η_2^i, $e_{x,1}^i$, and $e_{x,2}^i$, the dynamics of DGU i is written as

$$\begin{aligned}\dot{e}_{x,1}^i &= e_{x,2}^i\\ \dot{e}_{x,2}^i &= -\phi_1^i e_{x,1}^i - \phi_2^i e_{x,2}^i - \phi_3^i\mathcal{L}_i e_{x,1} - \phi_4^i\mathcal{L}_i e_{x,2}\\ &\quad + \eta_1^i + (g_1^i\bar{\phi}_1/\bar{g}_1 - \bar{\phi}_1)V_{\text{ref}} - g_2^i I_L^i - \tilde{\phi}_1^i\bar{x}_1 - \tilde{\phi}_2^i\bar{x}_2\\ \tau\dot{\eta}_1^i &= \eta_2^i\\ \tau\dot{\eta}_2^i &= -\alpha_0\frac{g_1^i}{\bar{g}_1}\big(-\tilde{\phi}_1^i e_{x,1}^i - \tilde{\phi}_2^i e_{x,2}^i - \phi_3^i\mathcal{L}_i e_{x,1} - \phi_4^i\mathcal{L}_i e_{x,2}\\ &\quad + \eta_1^i + (g_1^i\bar{\phi}_1/\bar{g}_1 - \bar{\phi}_1)V_{\text{ref}} - g_2^i I_L^i - \tilde{\phi}_1^i\bar{x}_1 - \tilde{\phi}_2^i\bar{x}_2\big)\\ &\quad - \alpha_1\eta_2^i.\end{aligned}$$

Proof: From the definition of $e_{x,1}^i$ and $e_{x,2}^i$, the dynamics of $e_{x,1}^i$ follows trivially. Recalling (15) and applying the relations $x_1^i = e_{x,1}^i + \bar{x}_1$, $x_2^i = e_{x,2}^i + \bar{x}_2$, $x_1 = e_{x,1} + 1_n\bar{x}_1$, $x_2 = e_{x,2} + 1_n\bar{x}_2$, and $\mathcal{L}_i 1_n = 0$, one can derive

$$\begin{aligned}\dot{e}_{x,2}^i &= -\phi_1^i x_1^i - \phi_2^i x_2^i - \phi_3^i\mathcal{L}_i x_1 - \phi_4^i\mathcal{L}_i x_2\\ &\quad + g_1^i\, u_1^i - g_2^i I_L^i + \bar{\phi}_1\bar{x}_1 + \bar{\phi}_2\bar{x}_2 - \bar{\phi}_1 V_{\text{ref}}\\ &= -\phi_1^i e_{x,1}^i - \phi_2^i e_{x,2}^i - \phi_3^i\mathcal{L}_i e_{x,1} - \phi_4^i\mathcal{L}_i e_{x,2}\\ &\quad + \eta_1^i + (g_1^i\bar{\phi}_1/\bar{g}_1 - \bar{\phi}_1)V_{\text{ref}} - g_2^i I_L^i - \tilde{\phi}_1^i\bar{x}_1 - \tilde{\phi}_2^i\bar{x}_2.\end{aligned}$$

Now we derive the dynamics of η_1^i and η_2^i. By definition of η_1^i and η_2^i, we have

$$\begin{aligned}\tau\dot{\eta}_1^i &= \eta_2^i\\ \tau\dot{\eta}_2^i &= g_1^i\tau^2\left(\ddot{q}_1^i - \frac{\alpha_0}{\tau^2}\frac{1}{\bar{g}_1}\dot{x}_2^i\right).\end{aligned}$$

In order to express the term $\ddot{q}_1^i$ in terms of new coordinates, we compute by using (13) and (14)

$$\begin{aligned}\dot{q}_1^i &= -\frac{\alpha_1}{\tau}\frac{1}{g_1^i}\eta_1^i + q_2^i - \frac{\alpha_0}{\tau^2}\frac{\bar{\phi}_2}{\bar{g}_1}x_1^i\\ \dot{q}_2^i &= \frac{\alpha_0}{\tau^2}\frac{\bar{\phi}_1}{\bar{g}_1}V_{\text{ref}} - \frac{\alpha_0}{\tau^2}\frac{\bar{\phi}_1}{\bar{g}_1}x_1^i,\end{aligned} \tag{16}$$

from which it follows that

$$\begin{aligned}\ddot{q}_1^i &= -\frac{\alpha_1}{\tau}\frac{1}{g_1^i}\dot{\eta}_1^i + \dot{q}_2^i - \frac{\alpha_0}{\tau^2}\frac{\bar{\phi}_2}{\bar{g}_1}\dot{x}_1^i\\ &= -\frac{\alpha_1}{\tau^2 g_1^i}\eta_2^i - \frac{\alpha_0}{\tau^2\bar{g}_1}(\bar{\phi}_1 x_1^i + \bar{\phi}_2 x_2^i - \bar{\phi}_1\, V_{\text{ref}}).\end{aligned}$$

Hence, the dynamics of η_2^i can be derived as

$$\begin{aligned}\tau\dot{\eta}_2^i &= -\alpha_0\frac{g_1^i}{\bar{g}_1}(\bar{\phi}_1 x_1^i + \bar{\phi}_2 x_2^i + \dot{x}_2^i - \bar{\phi}_1\, V_{\text{ref}}) - \alpha_1\eta_2^i\\ &= -\alpha_0\frac{g_1^i}{\bar{g}_1}\big(-\tilde{\phi}_1^i x_1^i - \tilde{\phi}_2^i x_2^i - \phi_3^i\mathcal{L}_i x_1 - \phi_4^i\mathcal{L}_i x_2\\ &\quad + g_1^i u^i - g_2^i I_L^i - \bar{\phi}_1\, V_{\text{ref}}\big) - \alpha_1\eta_2^i.\end{aligned}$$

Finally, applying the same relations as in the proof for $\dot{e}^i_{x,2}$, it is not difficult to derive the result for $\dot{\eta}^i_2$, which completes the proof. □

Since $\lim_{t\to\infty}(\bar{x}_1(t), \bar{x}_2(t)) = (V_{\text{ref}}, 0)$, we consider $e_{\bar{x},1} = \bar{x}_1 - V_{\text{ref}}$ and $e_{\bar{x},2} = \bar{x}_2 - 0$. Then, the dynamics of the desired model and the closed-loop system of DGU i can be expressed by

$$\begin{aligned}
\dot{e}_{\bar{x},1} &= e_{\bar{x},2}\\
\dot{e}_{\bar{x},2} &= -\bar{\phi}_1 e_{\bar{x},1} - \bar{\phi}_2 e_{\bar{x},2}\\
\dot{e}^i_{x,1} &= e^i_{x,2}\\
\dot{e}^i_{x,2} &= -\phi^i_1 e^i_{x,1} - \phi^i_2 e^i_{x,2} - \phi^i_3 \mathcal{L}_i e_{x,1} - \phi^i_4 \mathcal{L}_i e_{x,2}\\
&\quad + \eta^i_1 + (g^i_1\bar{\phi}_1/\bar{g}_1 - \phi^i_1)V_{\text{ref}} - g^i_2 I^i_L - \tilde{\phi}^i_1 e_{\bar{x},1} - \tilde{\phi}^i_2 e_{\bar{x},2}\\
\tau\dot{\eta}^i_1 &= \eta^i_2\\
\tau\dot{\eta}^i_2 &= -\alpha_0\frac{g^i_1}{\bar{g}_1}\big(- \tilde{\phi}^i_1 e^i_{x,1} - \tilde{\phi}^i_2 e^i_{x,2} - \phi^i_3 \mathcal{L}_i e_{x,1} - \phi^i_4 \mathcal{L}_i e_{x,2}\\
&\quad + \eta^i_1 + (g^i_1\bar{\phi}_1/\bar{g}_1 - \phi^i_1)V_{\text{ref}} - g^i_2 I^i_L - \tilde{\phi}^i_1 e_{\bar{x},1} - \tilde{\phi}^i_2 e_{\bar{x},2}\big)\\
&\quad - \alpha_1\eta^i_2. \qquad (17)
\end{aligned}$$

To proceed, we define vectors $\eta_1 = \big[\eta^1_1 \cdots \eta^n_1\big]$, $\eta_2 = \big[\eta^1_2 \cdots \eta^n_2\big]$, $I_L = \big[I^1_L \cdots I^n_L\big]^\top$. In addition, define $\Phi_j = diag\{\phi^1_j, \ldots, \phi^n_j\}$, $\tilde{\Phi}_j = diag\{\tilde{\phi}^1_j, \ldots, \tilde{\phi}^n_j\}$, for $j = 1, \ldots, 4$, and $G_1 = diag\{g^1_1, \ldots, g^n_1\}$, $G_2 = diag\{g^1_2, \ldots, g^n_2\}$. Then, using (17) and the definition of the vectors and the matrices, the dynamics of the whole closed-loop system is obtained as

$$\begin{aligned}
\dot{e}_{\bar{x},1} &= e_{\bar{x},2}\\
\dot{e}_{\bar{x},2} &= -\bar{\phi}_1 e_{\bar{x},1} - \bar{\phi}_2 e_{\bar{x},2}\\
\dot{e}_{x,1} &= e_{x,2}\\
\dot{e}_{x,2} &= -(K_1 + \bar{\phi}_1 I_n)e_{x,1} - (K_2 + \bar{\phi}_2 I_n)e_{x,2} + \eta_1\\
&\quad + K_3 1_n V_{\text{ref}} - G_2 I_L - \tilde{\Phi}_1 1_n e_{\bar{x},1} - \tilde{\Phi}_2 1_n e_{\bar{x},2}\\
\tau\dot{\eta}_1 &= \eta_2\\
\tau\dot{\eta}_2 &= -\frac{\alpha_0}{\bar{g}_1}G_1\big(- K_1 e_{x,1} - K_2 e_{x,2} + \eta_1 + K_3 1_n V_{\text{ref}}\\
&\quad - G_2 I_L - \tilde{\Phi}_1 1_n e_{\bar{x},1} - \tilde{\Phi}_2 1_n e_{\bar{x},2}\big) - \alpha_1\eta_2 \qquad (18)
\end{aligned}$$

where $K_1 = \tilde{\Phi}_1 + \Phi_3\mathcal{L}$, $K_2 = \tilde{\Phi}_2 + \Phi_4\mathcal{L}$, and $K_3 = (\bar{\phi}_1/\bar{g}_1)G_1 - \Phi_1$.

Remark 1: From the singular perturbation theory, if the design parameter τ is chosen sufficiently small, the dynamics of η_j is much faster than $e_{\bar{x},j}$ and $e_{x,j}$. Hence, the fast variable η_j converges to η^*_j, which is called the quasi-steady-state value, while the slow variables $e_{\bar{x},j}$ and $e_{x,j}$ are regarded as a fixed parameters. It is obtained by considering the dynamics of η_j in a stretched time scale $\bar{t} = t/\tau$ and taking $\tau \to 0$.

In view of Remark 1, we define η^*_j as

$$\begin{aligned}
\eta^*_1 &= K_1 e_{x,1} + K_2 e_{x,2} - K_3 1_n V_{\text{ref}} + G_2 I_L\\
&\quad + \tilde{\Phi}_1 1_n e_{\bar{x},1} + \tilde{\Phi}_2 1_n e_{\bar{x},2}\\
\eta^*_2 &= 0.
\end{aligned}$$

Then, we rewrite the error dynamics of the whole closed-loop system (18) using $e_{\eta,1} = \eta_1 - \eta^*_1$ and $e_{\eta,2} = \eta_2 - \eta^*_2$

$$\begin{aligned}
\dot{e}_{\bar{x},1} &= e_{\bar{x},2}\\
\dot{e}_{\bar{x},2} &= -\bar{\phi}_1 e_{\bar{x},1} - \bar{\phi}_2 e_{\bar{x},2}\\
\dot{e}_{x,1} &= e_{x,2}\\
\dot{e}_{x,2} &= -\bar{\phi}_1 e_{x,1} - \bar{\phi}_2 e_{x,2} + e_{\eta,1}\\
\dot{e}_{\eta,1} &= \bar{\phi}_1\tilde{\Phi}_2 1_n e_{\bar{x},1} - (\tilde{\Phi}_1 - \bar{\phi}_2\tilde{\Phi}_2)1_n e_{\bar{x},2} + \bar{\phi}_1 K_2 e_{x,1}\\
&\quad - (K_1 - \bar{\phi}_2 K_2)e_{x,2} - K_2 e_{\eta,1} + \frac{1}{\tau}e_{\eta,2}\\
\dot{e}_{\eta,2} &= -\frac{1}{\tau}\frac{\alpha_0}{\bar{g}_1}G_1 e_{\eta,1} - \frac{1}{\tau}\alpha_1 e_{\eta,2}. \qquad (19)
\end{aligned}$$

To proceed further, we define $e_{\bar{x}} = \big[e_{\bar{x},1}\ e_{\bar{x},2}\big]^\top$, $e_x = \big[e^\top_{x,1}\ e^\top_{x,2}\big]^\top$, $e_\eta = \big[e^\top_{\eta,1}\ e^\top_{\eta,2}\big]^\top$, and compactly rewrite the dynamics of (19) as

$$\begin{bmatrix}\dot{e}_{\bar{x}}\\ \dot{e}_x\\ \dot{e}_\eta\end{bmatrix} = \begin{bmatrix}A_{11} & 0 & 0\\ 0 & A_{22} & A_{23}\\ A_{31} & A_{32} & \tilde{A}_{33} + \frac{1}{\tau}A_{33}\end{bmatrix}\begin{bmatrix}e_{\bar{x}}\\ e_x\\ e_\eta\end{bmatrix} \qquad (20)$$

where

$$\begin{aligned}
A_{11} &= \begin{bmatrix}0 & 1\\ -\bar{\phi}_1 & -\bar{\phi}_2\end{bmatrix},\quad A_{22} = A_{11}\otimes I_n,\ A_{23} = \begin{bmatrix}0 & 0\\ I_n & 0\end{bmatrix},\\
A_{31} &= \begin{bmatrix}\bar{\phi}_1\tilde{\Phi}_2 1_n & -(\tilde{\Phi}_1 - \bar{\phi}_2\tilde{\Phi}_2)1_n\\ 0 & 0\end{bmatrix},\\
A_{32} &= \begin{bmatrix}\bar{\phi}_1 K_2 & -(K_1 - \bar{\phi}_2 K_2)\\ 0 & 0\end{bmatrix},\\
\tilde{A}_{33} &= \begin{bmatrix}-K_2 & 0\\ 0 & 0\end{bmatrix},\quad A_{33} = \begin{bmatrix}0 & I_n\\ -\frac{\alpha_0}{\bar{g}_1}G_1 & -\alpha_1 I_n\end{bmatrix}.
\end{aligned}$$

The stability of the closed-loop system can be determined if the system matrix of (20) is Hurwitz. Fortunately, the matrices A_{11}, A_{22}, and A_{33} that are located on the diagonal position are all Hurwitz since all the system parameters are positive, and the design parameters α_0, α_1, and τ will be chosen as positive numbers. In addition, the dynamics of $e_{\bar{x}}$ is standalone, it is sufficient to investigate the stability of (e_x, e_η). One notable observation is that the matrices A_{22}, A_{23}, A_{32}, and $\tilde{A}_{33}$ are fixed and only A_{33} contains the design parameters α_0, α_1, and τ. On the other hand, we have uncertainties in A_{32}, $\tilde{A}_{33}$, and A_{33} and this means that the interaction between e_x and e_η has uncertainties and this is the main obstacle to design stabilizing controller. Our strategy is to find a Lyapunov function for A_{33} that is independent of parameter uncertainty in G_1 and choose τ considering the interaction between e_x and e_η.

The following result addresses the stability of A_{33} using absolute stability [21].

Lemma 2: Let $g^-_1 = 1/(L_{\max}C_{\max})$ and $g^+_1 = 1/(L_{\min}C_{\min})$. Consider the system

$$\dot{\mathsf{e}} = A_{33}\mathsf{e} = \begin{bmatrix}0 & I_n\\ -\frac{\alpha_0}{\bar{g}_1}G_1 & -\alpha_1 I_n\end{bmatrix}\mathsf{e}. \qquad (21)$$

There exist a symmetric positive definite matrix P_η that is independent of G_1 and a constant $\epsilon > 0$ such that the functional $\mathcal{V}_\eta = \mathsf{e}^\top P_\eta \mathsf{e}$ satisfies

$$\dot{\mathcal{V}}_\eta \le -\epsilon \mathsf{e}^\top P_\eta \mathsf{e}$$

provided that α_0 and α_1 are chosen such that

$$\alpha_1 > \sqrt{\frac{\alpha_0}{\bar{g}_1}}\left(\sqrt{g_1^+} - \sqrt{g_1^-}\right). \tag{22}$$

Proof: The system (21) can be regarded as a feedback system given by

$$\begin{aligned}
\dot{\mathsf{e}} &= \begin{bmatrix} 0 & I_n \\ -\dfrac{\alpha_0}{\bar{g}_1} g_1^- I_n & -\alpha_1 I_n \end{bmatrix} \mathsf{e} + \begin{bmatrix} 0 \\ \dfrac{\alpha_0}{\bar{g}_1} I_n \end{bmatrix} u =: A\mathsf{e} + Bu \\
y &= \begin{bmatrix} I_n & 0 \end{bmatrix} \mathsf{e} + 0\, u =: C\mathsf{e} + Du \\
u &= -(G_1 - g_1^- I_n) y =: -\psi(y).
\end{aligned} \tag{23}$$

It is noted that $\psi(\cdot)$ is an uncertain function that belongs to the sector $[0, (g_1^+ - g_1^-)I_n]$ [21], i.e.,

$$\psi^\top(y)(\psi(y) - (g_1^+ - g_1^-)y) \le 0, \quad \forall y \in \mathbb{R}^n.$$

Let $H(s) = C(sI - A)^{-1}B + D$ be the transfer function of the system (23). It is noted that

$$H(s) = h(s) I_n, \quad h(s) = \frac{\alpha_0/\bar{g}_1}{s^2 + \alpha_1\, s + (\alpha_0/\bar{g}_1) g_1^-}.$$

One can compute that

$$\mathrm{Re}\{h(j\omega)\} = \frac{-(\alpha_0/\bar{g}_1)\omega^2 + (\alpha_0/\bar{g}_1)^2 g_1^-}{\omega^4 + (\alpha_1^2 - 2\alpha_0\, g_1^-/\bar{g}_1)\omega^2 + (\alpha_0\, g_1^-/\bar{g}_1)^2},$$

and find that the Nyquist plot of $h(s)$ is bounded to the negative real axis and the minimum of $\mathrm{Re}\{h(j\omega)\}$ is given by $-\alpha_0 / \left(2\alpha_1\sqrt{\alpha_0 \bar{g}_1 g_1^-} + \bar{g}_1 \alpha_1^2\right)$ at $\omega = \pm\sqrt{\alpha_0\, g_1^-/\bar{g}_1 + \alpha_1\sqrt{\alpha_0 g_1^-/\bar{g}_1}}$. Hence,

$$\min_\omega \mathrm{Re}\{h(j\omega)\} = \frac{-\alpha_0}{\bar{g}_1\left(\alpha_1 + \sqrt{\alpha_0\, g_1^-/\bar{g}_1}\right)^2 - \alpha_0 g_1^-},$$

and the condition (22) ensures that

$$\min_\omega \mathrm{Re}\{h(j\omega)\} > -(g_1^+ - g_1^-)^{-1},$$

equivalently, $\bar{H}(s) = (g_1^+ - g_1^-)h(s)I_n + I_n$ is strictly positive real.

Recalling that $H(s) = C(sI - A)^{-1}B + D$, a minimal realization of $\bar{H}(s)$ is given by

$$\begin{aligned}
\dot{\bar{e}} &= A\bar{e} + B\bar{u} \\
\bar{y} &= (g_1^+ - g_1^-)C\bar{e} + I_n\bar{u} =: \bar{C}\bar{e} + \bar{D}\bar{u}.
\end{aligned}$$

Since $\bar{H}(s)$ is strictly positive real, from Kalman-Yakubovich-Popov Lemma [21, Lemma 6.3], there exist a symmetric positive definite matrix P_η, matrices L and W, and a positive constant $\epsilon > 0$ such that

$$P_\eta A + A^\top P_\eta = -L^\top L - \epsilon P_\eta \tag{24a}$$

$$P_\eta B = \bar{C}^\top - L^\top W \tag{24b}$$

$$W^\top W = \bar{D} + \bar{D}^\top. \tag{24c}$$

Let $\mathcal{V}_\eta = \mathsf{e}^\top P_\eta \mathsf{e}$. Applying (24a) and (24b), we compute

$$\begin{aligned}
\dot{\mathcal{V}}_\eta &= \mathsf{e}^\top(P_\eta A + A^\top P_\eta)\mathsf{e} + 2\mathsf{e}^\top P_\eta B u \\
&= -\epsilon \mathsf{e}^\top P_\eta \mathsf{e} - \mathsf{e}^\top L^\top L \mathsf{e} + 2\mathsf{e}^\top(\bar{C}^\top - L^\top W)u \\
&= -\epsilon \mathsf{e}^\top P_\eta \mathsf{e} - \mathsf{e}^\top L^\top L \mathsf{e} - 2\mathsf{e}^\top L^\top W u - 2u^\top \bar{D}^\top u \\
&\quad + 2(\bar{C}\mathsf{e} + \bar{D}u)^\top u.
\end{aligned}$$

From (24c), we have

$$\dot{\mathcal{V}}_\eta = -\epsilon \mathsf{e}^\top P_\eta \mathsf{e} - \|L\mathsf{e} + Wu\|^2 + 2(\bar{C}\mathsf{e} + \bar{D}u)^\top u.$$

Finally, the relation $(\bar{C}\mathsf{e} + \bar{D}u)^\top u = -y^\top(g_1^+ I_n - G_1)(G_1 - g_1^- I_n)y$ results in

$$\dot{\mathcal{V}}_\eta \le -\epsilon \mathsf{e}^\top P_\eta \mathsf{e},$$

which completes the proof. □

With α_0 and α_1 chosen from Lemma 2, it remains to determine τ, which is explained below. Let $P_{\bar{x}} = P_{\bar{x}}^\top > 0$ and $P_x = P_x^\top > 0$ be the solutions of

$$\begin{aligned}
P_{\bar{x}} A_{11} + A_{11}^\top P_{\bar{x}} &= -I_2 \\
P_x A_{22} + A_{22}^\top P_x &= -I_{2n}.
\end{aligned} \tag{25}$$

It is noted that the existence is guaranteed because A_{11} and A_{22} are Hurwitz. Define

$$\begin{aligned}
\tilde{A}_1 &= 2A_{31}^\top P_\eta \\
\tilde{A}_2 &= 2P_x A_{23} + 2A_{32}^\top P_\eta \\
\tilde{A}_3 &= P_\eta \tilde{A}_{33} + \tilde{A}_{33}^\top P_\eta \\
M &= \frac{1}{2}\tilde{A}_1^\top \tilde{A}_1 + \frac{1}{2}\tilde{A}_2^\top \tilde{A}_2 + \tilde{A}_3.
\end{aligned} \tag{26}$$

It is noted that M is unknown but all the parameters are bounded (Assumption 1). Hence, we can find $\bar{m} > 0$ such that $M \le \bar{m} I$. Finally, choose τ such that

$$-\frac{\epsilon}{\tau}\lambda_{\min}(P_\eta) + \bar{m} \le -\frac{1}{2}. \tag{27}$$

Now, we are ready to present the main result of this paper.

Theorem 1: Suppose that Assumption 1 holds true and that controller parameters α_0, α_1, and τ are chosen according to (22) and (27). Then, the proposed controller (13) ensures that all signals in the closed-loop system are bounded and that

$$\lim_{t\to\infty} x_1^i(t) = \lim_{t\to\infty} \bar{x}_1(t) = V_{\mathrm{ref}}, \quad i = 1, \ldots, n.$$

Proof: Consider the Lyapunov function candidate

$$\mathcal{V} = e_{\bar{x}}^\top P_{\bar{x}} e_{\bar{x}} + e_x^\top P_x e_x + e_\eta^\top P_\eta e_\eta.$$

Using Lemma 2 and (25), we compute

$$\begin{aligned}
\dot{\mathcal{V}} \le &-\|e_{\bar{x}}\|^2 - \|e_x\|^2 - \frac{\epsilon}{\tau} e_\eta^\top P_\eta e_\eta + e_{\bar{x}}^\top \tilde{A}_1 e_\eta + e_x^\top \tilde{A}_2 e_\eta \\
&+ e_\eta^\top \tilde{A}_3 e_\eta
\end{aligned}$$

where $\tilde{A}_1$, $\tilde{A}_2$, and $\tilde{A}_3$ are defined in (26).

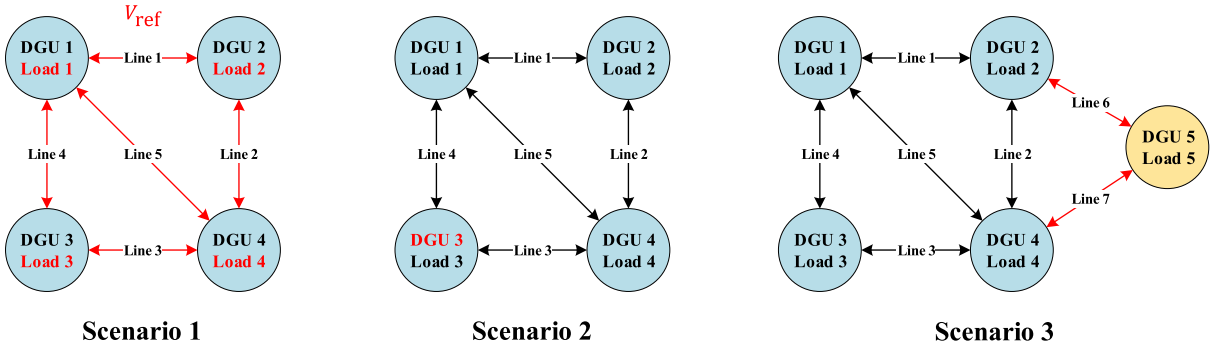

FIGURE 3. The configurations of the DC microgrid implemented in Scenario 1, 2, and 3, respectively. Changed elements are colored red.

Applying Young's inequality and recalling the definition of M, we have

$$\dot{\mathcal{V}} \leq -\frac{1}{2}\|e_{\bar{x}}\|^2 - \frac{1}{2}\|e_x\|^2 - \frac{\epsilon}{\tau}\lambda_{\min}(P_\eta)\|e_\eta\|^2 + e_\eta^\top M e_\eta.$$

From (27), it follows that

$$\dot{\mathcal{V}} \leq -\frac{1}{2}\|e_{\bar{x}}\|^2 - \frac{1}{2}\|e_x\|^2 - \frac{1}{2}\|e_\eta\|^2 \leq -\frac{1}{\delta}\mathcal{V}$$

where $\delta = \frac{1}{2}\min\left\{\frac{1}{\lambda_{\max}(P_{\bar{x}})}, \frac{1}{\lambda_{\max}(P_x)}, \frac{1}{\lambda_{\max}(P_\eta)}\right\}$.

Finally, by the comparison lemma, we have

$$\mathcal{V}(t) \leq e^{-\frac{1}{\delta}t}\mathcal{V}(0), \quad t \geq 0.$$

This means that all the signals in the closed-loop system are bounded and that

$$\lim_{t\to\infty} x_1^i(t) = \lim_{t\to\infty} \bar{x}_1(t) = V_{\text{ref}}, \quad i = 1, \ldots, n,$$

which completes the proof. □

IV. NUMERICAL SIMULATION

In this section, we study the performance of the proposed voltage stabilization controller described in Section III. Three scenarios are considered and they are illustrated in Fig. 3. In Scenarios 1 and 2, we consider a DC microgrid composed of 4 DGUs interconnected with 5 power lines. In Scenario 1, we evaluate the performance in terms of: 1) tracking voltage reference during initial period; 2) transients after the connection of 4 DGUs; 3) robustness of the voltage reference change; and 4) robustness of the current load changes. Next, in Scenario 2, we present the convergence performance of the proposed controller. We also compare with the proposed controller and the one from [15] when DGU 3 is changed. In Scenario 3, we investigate the Plug and Play capability of the proposed controller by considering that new DGU 5 is connected/disconnected to DGUs 2 and 4. The parameters of DGUs and power lines, and the values of current loads are summarized in Tables 1 and 2. Regarding Assumption 1, we assume that the parameters belong to known bounded sets; $R^i \in [0.1, 0.5], L^i \in [0.001, 0.003]$, and $C^i \in [0.001, 0.003]$. It is assumed that the control input u^i is saturated so that $u^i \in [0, 100]$.

TABLE 1. DGU parameters and current demands.

DGU i	1	2	3	4	5
R^i [Ω]	0.3	0.5	0.2	0.1	0.4
L^i [mH]	2.5	1.7	2.0	1.4	2.3
C^i [mF]	1.9	2.3	2.8	1.6	2.2
I_L^i [A]	4	6	2	8	5

TABLE 2. Power line parameters.

Line k	1	2	3	4	5	6	7
R^k [mΩ]	71	100	64	96	53	50	82
L^k [μH]	1.8	1.0	1.4	1.5	2.0	1.7	1.1

A. SCENARIO 1

Consider a DC microgrid composed of four DGUs connected through power lines (Fig. 3. Scenario 1). The voltage reference is selected as $V_{\text{ref}} = 48$ V, and the controller parameters are selected as $\alpha_0 = 10^3$, $\alpha_1 = 3 \times 10^4$, $\bar{\phi}_1 = 2.5 \times 10^3$, $\bar{\phi}_2 = 10^2$, $\bar{g}_1 = 1$, and $\tau = 10^{-4}$.

1) VOLTAGE REFERENCE TRACKING DURING INITIAL PHASE

During the initial time interval 0 s$\leq t \leq$ 2 s, the converters operate standalone and the controller tries to steer the output voltage to the reference value. As can be seen from Fig. 4 and Fig. 5, the output voltage of each DGU converges to its reference rapidly despite the presence of unknown local current load.

2) NEW CONNECTION OF THE DGU 1, 2, 3, AND 4

At $t = 2$ s, all DGUs are connected to the DC microgrid. Since the output voltages of DGUs reached the desired value, no significant transient can be observed; see Figs. 4, 5, and 6. This is mainly because the proposed controller is an output feedback controller (it requires only the output V^i) and the voltage difference between DGUs mainly affects the dynamics (4).

3) STEP CHANGE OF THE VOLTAGE REFERENCE

The response of the closed-loop system under step change of the voltage reference (V_{ref}) is illustrated. The voltage reference is reduced to 50% of its initial value (i.e., $V_{\text{ref}} = 48 \rightarrow 24$ V) at $t = 4$ s, the response is redrawn in Fig. 7 around

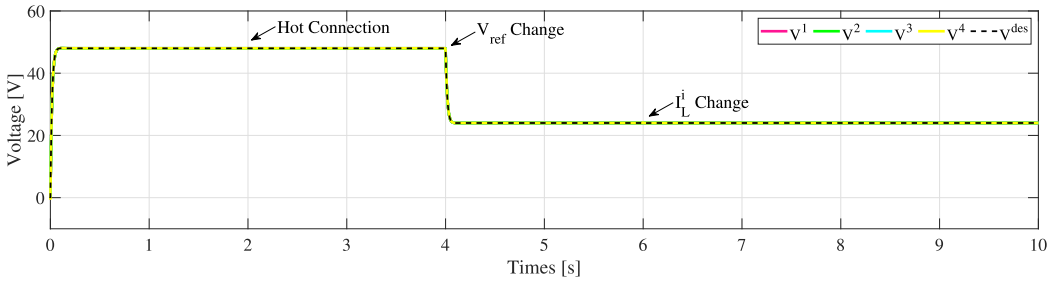

FIGURE 4. Scenario 1 - The output voltages of four DGUs and its reference (dashed line).

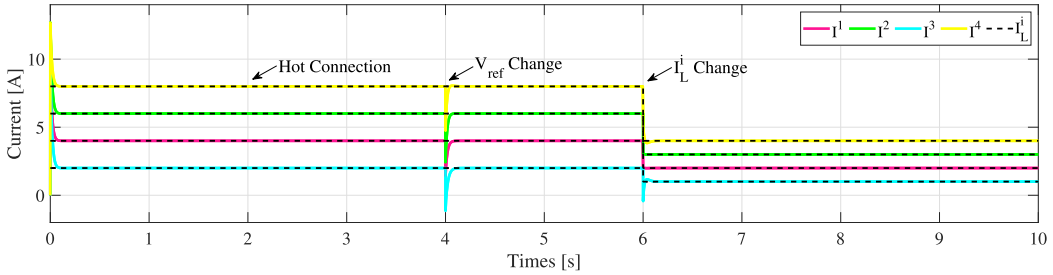

FIGURE 5. Scenario 1 - The output currents of four DGUs and the local current loads (dashed lines).

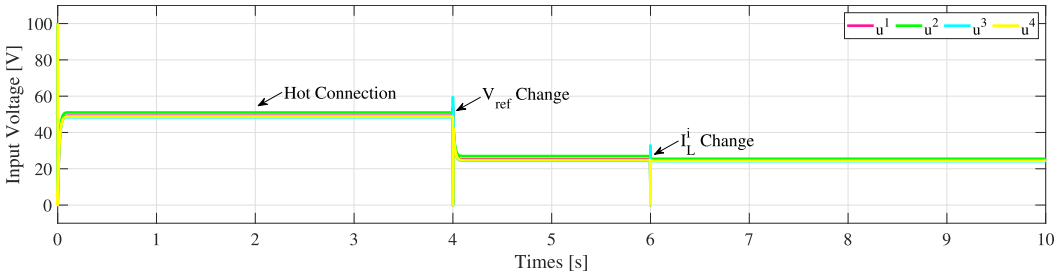

FIGURE 6. Scenario 1 - The control inputs of four DGUs.

$t = 4$ s. It can be seen that the output voltage of each DGU converges to its new reference in 0.1 s. The current of each DGU experiences a drop but recovers so that the current load demand is satisfied in the steady state.

4) CHANGE OF UNKNOWN CURRENT LOAD

We also present the performance of the controller when all current loads are decreased to half of their initial values (see Table 1) at $t = 6$ s. The response around $t = 6$ s is zoomed in Fig. 8. Fig. 8(a) shows that the output voltage of each DGU converges to its reference after a slight overshoot. Fig. 8(b) shows a good compensation of the current disturbances produced by the load change.

B. SCENARIO 2

1) TUNABLE DESIRED MODEL

One of important benefits of proposed controller is that the desired model can be freely chosen and the behavior of each DGU is approximately the same as the desired one. This is because the proposed controller estimates the discrepancy between the desire model and the real model and generates a compensating control signal. In order to illustrate this property, we choose two desired models: fast model (V_f^{des}) with $\bar{\phi}_1 = 2.5 \times 10^3$ and $\bar{\phi}_2 = 10^2$, and slow model (V_s^{des}) with $\bar{\phi}_1 = 50$ and $\bar{\phi}_2 = 15$. It is noted that we do not need to redesign the parameters of controllers and they are fixed as $\alpha_0 = 10^3$, $\alpha_1 = 3 \times 10^4$, $\bar{g}_1 = 1$, and $\tau = 10^{-4}$. The voltage reference is changed from 48 V to 24 V at $t = 4$ s. Fig. 9 shows the output voltages and the output currents of all DGUs around $t = 4$ s. In Fig. 9(a), two groups of the responses can be seen, the responses of one group converge to the new voltage reference very fast (lower responses, convergence time less than 0.1 s) while those of the other group converge relatively slowly. In both groups, the responses are almost identical to the desired model and this implies that the convergence performance of DGUs can be freely assignable through the desired model without further tuning of controller parameters α_0, α_1, and τ. In Fig. 9(b), all controllers satisfy the demands of the current load, although they have different desired models.

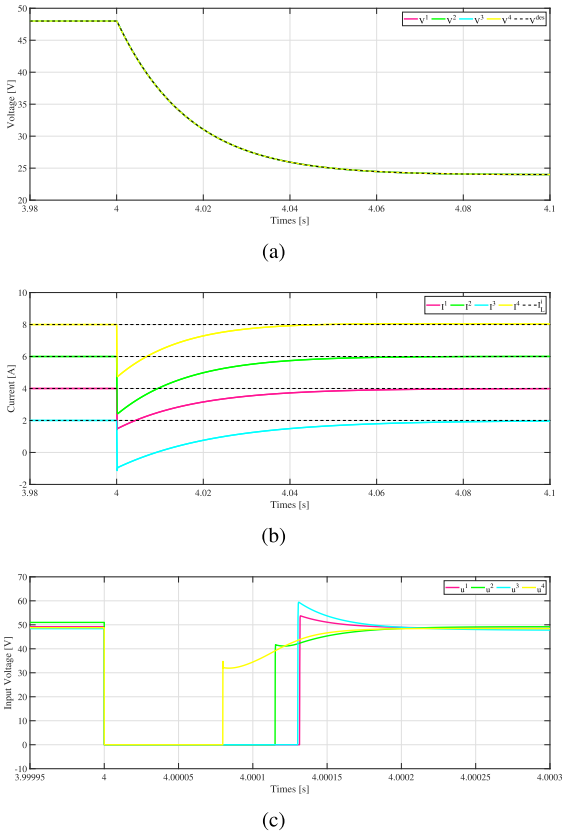

FIGURE 7. Scenario 1 - Voltage reference change. (a) The output voltage of each DGU and the trajectory of the desired voltage model (dashed line); (b) The output current of each DGU together with the current load demands (dashed lines); (c) The control inputs.

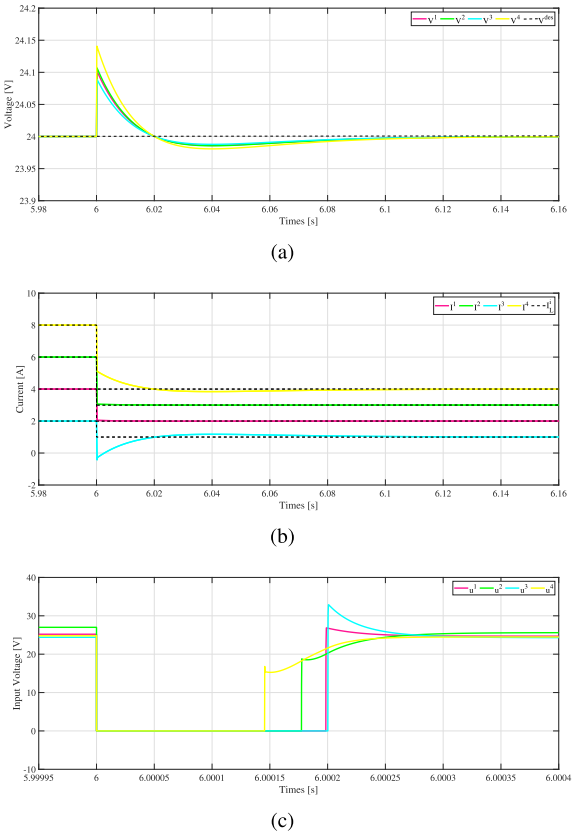

FIGURE 8. Scenario 1 - Unknown current load change. (a) The output voltage of each DGU and the trajectory of the desired voltage model (dashed line); (b) The output current of each DGU together with the current load demands (dashed lines); (c) The control inputs.

2) ROBUSTNESS AGAINST DGU PARAMETER CHANGE

Next, we compare the proposed controller and the one from [15] in terms of robustness against model change. At $t = 6$ s, the voltage reference is changed from 48 V to 24 V, and the parameters of DGU 3 are changed to $R^3 = 0.4\Omega$, $L^3 = 1.0$ mH, and $C^3 = 1.4$ mF. Note that we change the parameters of DGU 3 within the boundaries of R^i, L^i, and C^i. The parameters of the proposed controller are the same as Scenario 1 and those of [15] are chosen as $k_{1,i} = \frac{10}{11}$, $k_{2,i} = \frac{R^i}{10}$, and $k_{3,i} = \frac{2}{5L^i}(k_{1,i} - 1)(k_{2,i} - R^i)$.

Fig. 10 shows the output voltages of DGUs under the proposed controller and that of [15] when the parameters of DGU 3 change. Note that the blue and red lines are the output voltages of DGUs before and after the change of DGU 3 parameters, respectively. Although all of the output voltages converge to the voltage reference successfully, the output voltages of DGUs under the proposed controller remain almost the same in spite of the parameter change while a significant difference is observed under the other controller.

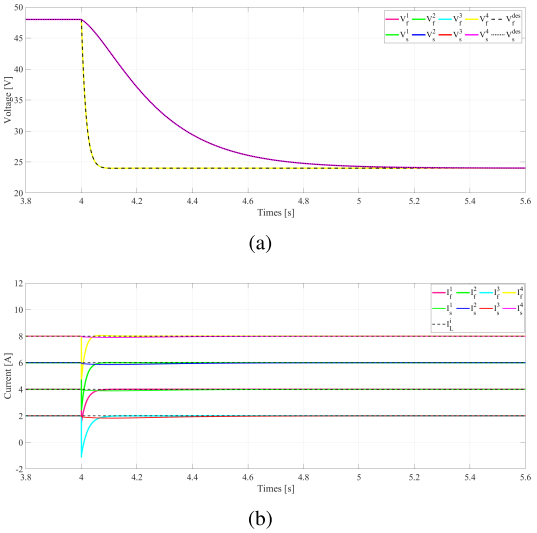

FIGURE 9. Scenario 2 - Tunable desired model. (a) The output voltages of all DGUs for the fast desired model (V_f^{des}) and the slow one (V_s^{des}); (b) The output currents of all DGUs for the fast desired model and the slow one and the current load demands (dashed lines).

C. SCENARIO 3

In this scenario, we investigate the PnP capabilities of the proposed controller. As can be seen in Fig. 3 (Scenario 3), four DGUs are initially connected and a new DGU 5 is connected to DGUs 2 and 4 at $t = 4$ s, and it is disconnected at $t = 6$ s. In order to allow current flow through the power lines, we set slightly different voltage references for the DGUs (see Table 3) as in the work [13]. The controller

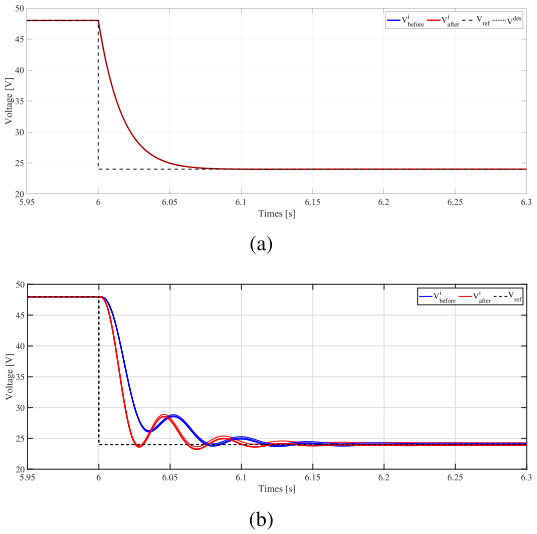

FIGURE 10. Scenario 2 - Robustness against DGU parameter change. the output voltages with no change of parameters (blue lines), with change of parameters in DGU 3 (red lines), its reference (dashed line), and the desired voltage model (densely dashed line) (a) Proposed controller; (b) The controller from [15].

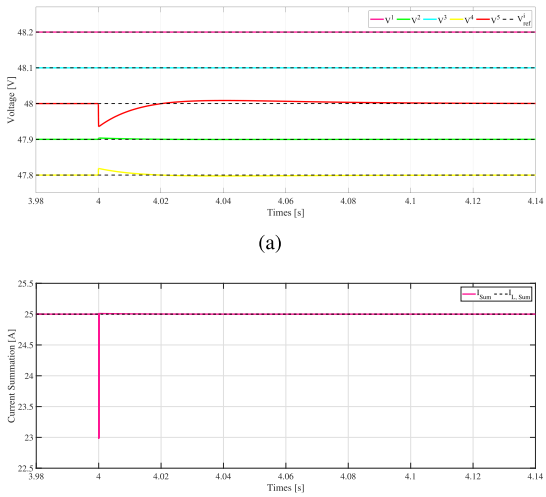

FIGURE 11. Scenario 3 - Plug-in of DGU 5 to DGUs 2 and 4. (a) The output voltage of each DGU and the voltage reference (dashed line); (b) The summations of the output currents of all DGUs and the summations of all current load demands (dashed lines).

TABLE 3. Voltage references for five DGUs.

DGU i	1	2	3	4	5
V^i_{ref} [V]	48.2	47.9	48.1	47.8	48.0

parameters are selected as $\alpha_0 = 10^3$, $\alpha_1 = 3 \times 10^4$, $\bar{\phi}_1 = 2.5 \times 10^3$, $\bar{\phi}_2 = 10^2$, $\bar{g}_1 = 1$, and $\tau = 10^{-4}$. Figs. 11 and 12 show the output voltages of DGUs and the sum of all output current connected to the microgrid Fig. 11(a) and Fig. 12(a) show that the output voltage of each DGU converges to the voltage reference. In particular, DGUs 2, 4, and 5, which are directly connected, have voltage variations, but

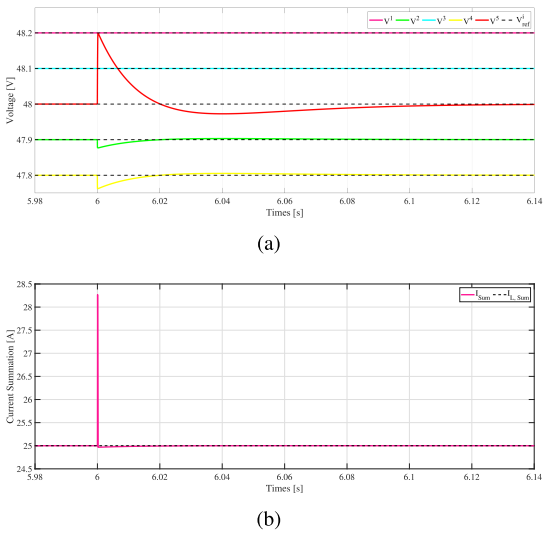

FIGURE 12. Scenario 3 - Unplugging of DGU 5 to DGUs 2 and 4. (a) The output voltage of each DGU and the voltage reference (dashed line); (b) The summations of the output currents of all DGUs and the summations of all current load demands (dashed lines).

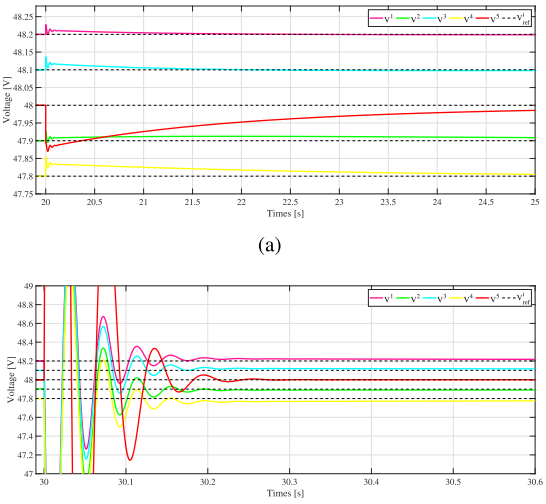

FIGURE 13. Scenario 3 - System behavior under the controller [15] in PnP situation. The output voltage of each DGU and the voltage reference (dashed line) (a) Plug-in (b) Unplugging.

DGUs 1 and 3 experience almost no deviation. Figs. 11(b) and 12(b) show the sum of output currents and the total current load. Although it has a current drop in a very short transient time interval, the sum of output currents successfully produce the desired total current. Next, we compare the performance of the controller [15] and the proposed controller in the PnP situation. Fig. 13(a) and Fig. 13(b) show the output voltage of each DGU and the voltage reference of the controller [15] in plug-in and unplugging, respectively. Large fluctuations are observed in the transient time interval. Moreover, unlike the proposed controller, this undesirable behavior is observed in DGUs 1 and 3 which are indirectly connected to DGU 5.

V. CONCLUSION

We have presented a new voltage stabilization controller for DC microgrids that are subject to unknown loads and model uncertainties. The proposed controller employs the disturbance observer based controller. It is shown that the proposed controller provides robustness against parameter uncertainties and unknown loads, and a constructive design procedure is presented. It is noted that the desired convergence rate of the voltage can be easily tuned without additional modification of controller parameters. For the whole closed-loop system including the proposed controller, a rigorous stability analysis is conducted and extensive simulation results are presented showing the effectiveness of the proposed controller. Our future work is to combine the proposed controller with higher level controller for achieving, e.g., proportional load sharing. We are also preparing a lab-scale experiment to validate the proposed controller.

REFERENCES

[1] D. E. Olivares, A. Mehrizi-Sani, A. H. Etemadi, C. A. Cañizares, R. Iravani, M. Kazerani, A. H. Hajimiragha, O. Gomis-Bellmunt, M. Saeedifard, R. Palma-Behnke, G. A. Jiménez-Estévez, and N. D. Hatziargyriou, "Trends in microgrid control," *IEEE Trans. Smart Grid*, vol. 5, no. 4, pp. 1905–1919, Jul. 2014.

[2] J. M. Guerrero, M. Chandorkar, T.-L. Lee, and P. C. Loh, "Advanced control architectures for intelligent microgrids—Part I: Decentralized and hierarchical control," *IEEE Trans. Ind. Electron.*, vol. 60, no. 4, pp. 1254–1262, Apr. 2013.

[3] J. M. Guerrero, P. C. Loh, T.-L. Lee, and M. Chandorkar, "Advanced control architectures for intelligent microgrids—Part II: Power quality, energy storage, and AC/DC microgrids," *IEEE Trans. Ind. Electron.*, vol. 60, no. 4, pp. 1263–1270, Apr. 2013.

[4] T. Dragičević, X. Lu, J. C. Vasquez, and J. M. Guerrero, "DC microgrids—Part I: A review of control strategies and stabilization techniques," *IEEE Trans. Power Electron.*, vol. 31, no. 7, pp. 4876–4891, Jul. 2016.

[5] T. Dragicevic, X. Lu, J. C. Vasquez, and J. M. Guerrero, "DC microgrids—Part II: A review of power architectures, applications, and standardization issues," *IEEE Trans. Power Electron.*, vol. 31, no. 5, pp. 3528–3549, May 2016.

[6] Y. Gu, W. Li, and X. He, "Frequency-coordinating virtual impedance for autonomous power management of DC microgrid," *IEEE Trans. Power Electron.*, vol. 30, no. 4, pp. 2328–2337, Apr. 2015.

[7] J. M. Guerrero, J. C. Vasquez, J. Matas, L. G. de Vicuna, and M. Castilla, "Hierarchical control of droop-controlled AC and DC microgrids—A general approach toward standardization," *IEEE Trans. Ind. Electron.*, vol. 58, no. 1, pp. 158–172, Jan. 2011.

[8] A. Bidram and A. Davoudi, "Hierarchical structure of microgrids control system," *IEEE Trans. Smart Grid*, vol. 3, no. 4, pp. 1963–1976, Dec. 2012.

[9] S. Anand, B. G. Fernandes, and J. Guerrero, "Distributed control to ensure proportional load sharing and improve voltage regulation in low-voltage DC microgrids," *IEEE Trans. Power Electron.*, vol. 28, no. 4, pp. 1900–1913, Apr. 2013.

[10] X. Lu, J. M. Guerrero, K. Sun, and J. C. Vasquez, "An improved droop control method for DC microgrids based on low bandwidth communication with DC bus voltage restoration and enhanced current sharing accuracy," *IEEE Trans. Power Electron.*, vol. 29, no. 4, pp. 1800–1812, Apr. 2014.

[11] V. Nasirian, A. Davoudi, F. L. Lewis, and J. M. Guerrero, "Distributed adaptive droop control for DC distribution systems," *IEEE Trans. Energy Convers.*, vol. 29, no. 4, pp. 944–956, Dec. 2014.

[12] V. Nasirian, S. Moayedi, A. Davoudi, and F. L. Lewis, "Distributed cooperative control of DC microgrids," *IEEE Trans. Power Electron.*, vol. 30, no. 4, pp. 2288–2303, Apr. 2015.

[13] M. Tucci, S. Riverso, J. C. Vasquez, J. M. Guerrero, and G. Ferrari-Trecate, "A decentralized scalable approach to voltage control of DC islanded microgrids," *IEEE Trans. Control Syst. Technol.*, vol. 24, no. 6, pp. 1965–1979, Nov. 2016.

[14] M. Tucci, S. Riverso, and G. Ferrari-Trecate, "Line-independent plug-and-play controllers for voltage stabilization in DC microgrids," *IEEE Trans. Control Syst. Technol.*, vol. 26, no. 3, pp. 1115–1123, May 2018.

[15] P. Nahata and G. Ferrari-Trecate, "On existence of equilibria, voltage balancing, and current sharing in consensus-based DC microgrids," in *Proc. Eur. Control Conf. (ECC)*, St. Petersburg, Russia, May 2020, pp. 1216–1223.

[16] S. Trip, M. Cucuzzella, X. Cheng, and J. Scherpen, "Distributed averaging control for voltage regulation and current sharing in DC microgrids," *IEEE Control Syst. Lett.*, vol. 3, no. 1, pp. 174–179, Jan. 2019.

[17] J. Lee and J. Back, "Robust distributed cooperative controller for DC microgrids with heterogeneous sources," *Int. J. Control, Autom. Syst.*, vol. 19, no. 2, pp. 736–744, Feb. 2021.

[18] K. Ohnishi, "A new servo method in mechatronics," *Trans. Jpn. Soc. Elect. Eng.*, vol. 107-D, no. 1, pp. 83–86, 1987.

[19] J. Back and H. Shim, "Adding robustness to nominal output-feedback controllers for uncertain nonlinear systems: A nonlinear version of disturbance observer," *Automatica*, vol. 44, no. 10, pp. 2528–2537, Oct. 2008.

[20] J. Back and H. Shim, "Reduced-order implementation of disturbance observers for robust tracking of non-linear systems," *IET Control Theory Appl.*, vol. 8, no. 17, pp. 1940–1948, Nov. 2014.

[21] H. K. Khalil, *Nonlinear Systems*, 3rd ed. Upper Saddle River, NJ, USA: Prentice-Hall, 2002.

JUWON LEE received the B.S. degree from the School of Robotics, Kwangwoon University, Seoul, South Korea, in 2015. He is currently pursuing the M.S./Ph.D. degree with Kwangwoon University. His research interests include control system theory, multi-agent systems, and dc microgrids.

HYO-SUNG AHN (Senior Member, IEEE) received the B.S. and M.S. degrees in astronomy from Yonsei University, Seoul, South Korea, in 1998 and 2000, respectively, the M.S. degree in electrical engineering from the University of North Dakota, Grand Forks, ND, USA, in 2003, and the Ph.D. degree in electrical engineering from Utah State University, Logan, UT, USA, in 2006. He is currently a Professor with the School of Mechanical Engineering, Gwangju Institute of Science and Technology (GIST), Gwangju, South Korea. His research interests include distributed control, aerospace navigation and control, network localization, and learning control.

JUHOON BACK (Member, IEEE) received the B.S. and M.S. degrees in mechanical design and production engineering from Seoul National University, Seoul, South Korea, in 1997 and 1999, respectively, and the Ph.D. degree from the School of Electrical Engineering and Computer Science, Seoul National University, in 2004. Since 2008, he has been with Kwangwoon University, South Korea, where he is currently a Professor. His research interests include control system theory and design, renewable energy systems, and multi-agent systems.